Catalysis Today 210 (2013) 89–97

Contents lists available at SciVerse ScienceDirect

Catalysis Today

journal homepage: www.elsevier.com/locate/cattod

Modelling of experimental vanillin hydrodeoxygenation reactions in water/oil emulsions. Effects of mass transport

M.T. Jimaré[a], F. Cazaña[a], A. Ramirez[a], C. Royo[a], E. Romeo[a], J. Faria[b], D.E. Resasco[b], A. Monzón[a,*]

[a] Department of Chemical and Environmental Engineering, Institute of Nanoscience of Aragón (INA), University of Zaragoza, Spain
[b] School of Chemical, Biological, and Materials Engineering, University of Oklahoma, USA

ARTICLE INFO

Article history:
Received 28 August 2012
Received in revised form 7 November 2012
Accepted 9 November 2012
Available online 1 February 2013

Keywords:
Nanohybrids
Mass transport coefficients
Vanillin
p-creosol
Hydrodeoxygenation
Pickering emulsion

ABSTRACT

We have studied the coupling of mass transport and chemical reaction rates in a biphasic emulsion system. The emulsion is stabilized by the presence of solid nanoparticles that, in addition, act as a catalyst for the reaction. These solid nanoparticles are composed of carbon nanotubes (CNTs) attached to SiO_2 nanoparticles. Both components, CNTs and silica, can be selectively impregnated by a catalytic active phase (e.g. Pd) forming the so-called *nanohybrids*. We have studied the application of the catalytic nanohybrids in emulsions of type (*w*/*o*), during the reaction of hydrodeoxygenation of vanillin (4-hydroxy-3-methoxybenzaldehyde). This is a model reaction that occurs in the aqueous side of the interface of the emulsion. The main target for this work is to analyze the impact of mass transport of the main compounds between the aqueous and organic phases on the global performance of the reaction.

1. Introduction

A major problem typically found in the upgrading of bio-oil is its low chemical stability due to the high reactivity of a large amount of oxygenated compounds present in this liquid. A possible solution to this problem is to deoxygenate some of the most active compounds present in the bio-oil [1,2]. However, this catalytic refining should be carried out in a complex system formed by two immiscible phases (aqueous and organic) and with a heterogeneous catalyst placed at the interface, obtaining a phase transport catalysis process [3–6].

To enhance the mass transport rate between the two phases, and therefore the global performance of the "bio-oil" refining process, it is necessary to increase both, the interfacial area between phases and the intrinsic rate of transport, i.e. the value of the transport coefficients. The formation of a stable emulsion helps increasing the interfacial surface area, which is where the reaction occurs if the catalysts particles are placed there [7]. Emulsions can be stabilized by addition of surfactants. However, one of the main drawbacks of these biphasic systems is that surfactants are difficult to separate and recover from the final mixture. On the contrary, solid particles are more easily recoverable than conventional surfactants, and have also been shown to stabilize aqueous–organic emulsions [8–16]. These emulsions stabilized by solids are called Pickering emulsions [17]. It has been recently shown [8,10] that the so-called "*nanohybrids*" of type CNT/SiO_2 can stabilize water-in-oil (*w*/*o*) and oil-in-water (*o*/*w*) emulsions. This behaviour is due to the amphiphilic character of thenanohybrids that contain a hydrophilic (SiO_2 support) and hydrophobic part (CNT). By impregnating the CNTs, Me/CNTs/Support, and/or the support, with metallic nanoparticles, the nanohybrids thus obtained are able to stabilize the emulsion and simultaneously, selectively catalyze reactions in organic phase or in aqueous phase [8,11].

It is well known that the driving force that determines chemical reaction and diffusion rates is given by thermodynamic properties, such as chemical affinity, chemical potential, or activity. Only in ideal reaction mixtures it is possible to express the reaction and mass transport rates as a function of the concentration of the species present in the system [18]. Specifically, in the case of catalytic reactions in gas–liquid–solid systems, reacting molecules are solvated and, in general, reside in a non-ideal environment. Madon et al. [19] pointed out that when the liquid and gas phases reach the thermodynamic equilibrium, the chemical potential of those phases becomes equal. Therefore, when the phases are equilibrated, the reaction rate should be independent of the location of the reactants and catalysts.

However, the concept of equal chemical potential does not apply when: (a) the phases are not in thermodynamic equilibrium, due to mass transport limitations, (b) the solvent competes with the reactant molecules for adsorption on the active sites [18–22], or (c)

* Corresponding author. Tel.: +34 976 761157.
E-mail addresses: amonzon@unizar.es, monzon.bescos@gmail.com (A. Monzón).

0920-5861/$ – see front matter © 2012 Elsevier B.V. All rights reserved.
http://dx.doi.org/10.1016/j.cattod.2012.11.015

the liquid does not solvate kinetically relevant adsorbed intermediates and activated complexes to the same extent. Hence, when the reactions are carried out in systems catalyzed by these nanohybrids placed at the interface of the emulsion, three important factors must be considered: (1) the formation and properties of the emulsion, (2) mass transport phenomena between the phases, and (3) the activity and selectivity of the reactions.

Although the properties and stabilization methods of emulsions have been extensively studied [9–11,23–32,16], the application of nanohybrids of the type Me/CNTs/support is a research topic of very recent development [8,10,33]. Likewise, there are numerous studies related to simultaneous mass transport and chemical reaction between two liquid phases [34,35], but the effect of mass transport in Pickering emulsions, where chemical reactions are carried out, has not been examined. In this work, we have examined the model reaction of hydrodeoxygenation of a vanillin with Pd/CNT/SiO_2 to investigate these combined effects in the application of the catalytic nanohybrids in the aqueous side of the interfaceof a *w*/*o* emulsion (water/decaline).

2. Materials and experimental methods

2.1. Materials

The oil used in the experiments was anhydrous decalin (decahydronaphthalene) provided by Sigma–Aldrich. Water was purified by circulating through two ion exchangers (Cole-Parmer Inc.). The reagents used were vanillin ((3-methoxy-4-hydroxybenzaldehyde), provided by Sigma–Aldrich, and p-creosol (2-methoxy-4-methyl phenol), provided by Alfa Aesar. Finally, hydrophobic silica particles (Aerosil R972) were provided by Evonik Industries.

2.2. Experimental methods

2.2.1. Preparation of the emulsions

Hydrophobic silica particles were dispersed in 10 mL of decalin and water mixture (ratio oil/water = 1). The liquid mixture plus the SiO_2 added was sonicated for 4 min at 20% amplitude (Ultrasonic Processors 750W). After sonication, the emulsion was stabilized for 24 h. Based on previous work [10], 0.2 wt.% of nanohybrids was used for the stabilization of the emulsions. The wt.% is defined as 100 × *g* of solid/g. of emulsion. In Refs. [8,10] there are detailed schemes of the formation of the emulsion and of the evolution of the existing phases.

2.2.2. High resolution electron microscopy with energy-dispersive X-ray spectroscopy (HRTEM-EDS)

Images and spectra were collected on a JEOL 2010-F field emission intermediate voltage (200,000 V) scanning transmission research electron microscope, with a magnification of up to 8,000,000× equipped with an EDS detector.

2.2.3. Experimental measurements for the case of single continuous interface

In this case, the experiments were realized without formation of emulsion and only mass transport across the continuous interface was observed. 5 mL of 0.1 M vanillin in water solution were added to 5 mL of decalin, using a vial of 20 mL total volume. The mixture was stirred at different rates (*rpm*) and temperatures. In the case of p-creosol, 5 mL of 0.005 M p-creosol in decaline was added to a vial with 5 mL water and the same factors were studied. The evolution with timeof the solute concentration (vanillin or p-creosol) in both phases was measured by GC–FID (GC Agilent 7890A) equipped with a capillary column of polyethylene glycol (HP-INNOWAX) of 60.0 m × 0.32 mm × 0.25 μm nominal from Hewlett Packard. The identification of the species was made by GC–MS (Shimadzu QP2010S) using a HP-INNOWAXpolyethylene glycolcapillary column, 30.0 m long × 0.25 μm nominal, from Hewlett Packard.

2.2.4. Experimental measurements for the case of stable emulsion

In these experiments, the emulsion was prepared as described above, using the same vials used for experiments with single continuous interface. 2 mL of a solution of 0.037 M vanillin (or p-creosol) in water were added to the vial and the mixture was stirred at 100 rpm and 25 °C. After that, the phases of oil free (i.e. out the emulsion) and water free (out the emulsion) were recovered and analysed by GC–FID. The remaining emulsion was filtered and the two phases obtained wereanalysed by GC–FID.

2.2.5. Catalytic conversion of vanillin

These experiments have been described previously [8]. Briefly, in each experiment, a mixture of 30 mg of nanohybrids and water was sonicated and the same volume of decaline was added to the reactor. After purge with nitrogen, the pressure was raised to 200 psi and the temperature to 100 °C. The catalyst is reduced for 3 h in hydrogen, then the reactants were added to the reactor and it was pressurized at 250 psi with hydrogen. The reactor was heated up to the reaction temperature and when this temperature was reached the reactants were feed and the reaction was started. To stop the reaction, the temperature was quickly dropped and the flow of hydrogen was replaced by nitrogen. After the reaction, the content of the reactor was filtered. Water and oil phase were separated and the samples were analysed by gas chromatography, GC–FID and GC–MS.

2.2.6. Modelling of mass transport phenomena and simultaneous reaction in emulsion

During the reaction of hydrodeoxygenation of vanillin on Pd/CNT/SiO_2 nanohybrids both the hydrophobic and hydrophilic sides contribute to the catalytic activity. However, to minimize the number of adjustable parameters and simplify the modelling we have assumed that the reaction takes place only on the aqueous phase. While this is an approximation, it is supported by HRTEM observations and EDS data that show that most of the Pd clusters are located on the hydrophilic oxide support (Fig. 1), due to the weak interaction of the metal nanoparticles with the pristine SWCNT in the hydrophobic side [36]. In addition to the conversion terms, the model takes into account the transport of all the species from one phase to the other. Accordingly, vanillin alcohol is produced inside the water droplets in the emulsion. Then, it partitions between the two phases and undergoes hydrogenolysis in the aqueous phase to p-creosol, which in turns also partitions between the phases [8].

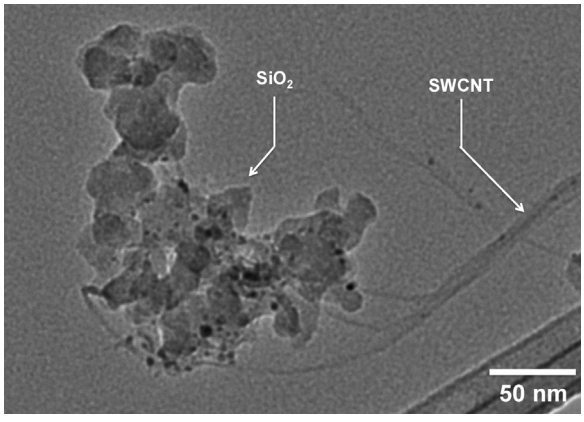

Fig. 1. HRTEM image of 5 wt.% Pd/SWCNT/SiO_2.

As a first step, we have studied the partition coefficientsof vanillin and p-creosol between the two phases, and the mass transport coefficients for two different cases: (1) a single continuous interface, and (2) a stable emulsion.

According to the double-layer theory (DLT), the mass transport rate of a solute A (e.g. vanillin or p-creosol) across a continuous interface water–oil can be expressed in terms of the overall mass transport coefficients as follows:

$$\frac{dC_A^{w}}{dt} = -(K_A^{w}a)(C_A^{w} - C_A^{w,*}) \quad (1)$$

$$\frac{dC_A^{o}}{dt} = (K_A^{o}a)(C_A^{o,*} - C_A^{o}); \quad C_A^{w,*} = H_A C_A^{o} \quad (2)$$

From the above equations and taking into account the global mass balance, in Appendix A.1it is shown that the evolution of the concentration of solute A in the oil phase with time can be given by:

$$C_A^{o} = C_{A_\infty}^{o}(1 - \exp(-(K_A^{o}a)_{eff}t)) \quad (3)$$

The thermodynamic and mass transport parameters, H_A, $(K_A^{o}a)$ and $(K_A^{w}a)$ are calculated from the fitting of the experimental data of A concentration in the oil phase with time to the above equation.

For the case of a stable emulsion, the phenomena involved during the mass transport is rather complex and therefore it has been described with empirical models. Two models have been proposed: (1) Potential model, (2) Exponential model.

The equations proposed for the *Potential Model* are:

$$\frac{dC_A^{f}}{dt} = -K_A^{f}(C_A^{f} - C_A^{f,s})^{n} \quad (4)$$

$$\frac{dC_A^{e}}{dt} = -K_A^{e}(C_A^{e,s} - C_A^{e})^{n} \quad (5)$$

It is assumed that the *order* of the *Potential Model*, n, is related to the number of mass transport phenomena (e.g. from free water to droplets of water inside the emulsion, from free water to oil of the emulsion, etc.) involved in the global process.

For example, in the case of $n = 2$ the evolution of the concentration of solute A with time in the free water and in the emulsion is given by:

$$C_A^{f} = C_A^{f,s} + \frac{(C_{A,0}^{f} - C_A^{f,s})}{(1 + k_{A,eff}^{f}t)} \quad (6)$$

$$C_A^{e} = C_A^{e,s} + \frac{(C_A^{e,s} - C_{A,0}^{e})}{(1 + k_{A,eff}^{e}t)} \quad (7)$$

Meanwhile, in the case of the *Exponential Model* the mass transport rate is described as a sum of exponential functions. In this model, the number of the exponentials, n, is related the number mass transport phenomena involved in the global process. Assuming again that $n = 2$ in this model, the evolution of the concentration of solute A in free water and in the emulsion is given by:

$$\begin{aligned} C_A^{f} &= C_{A_{1,0}}^{f}\exp(-k_{A_1}^{f}t) + C_{A_{2,0}}^{f}\exp(-k_{A_1}^{f}t) \\ C_{A_0}^{f} &= C_{A_{1,0}}^{f} + C_{A_{2,0}}^{f} \end{aligned} \quad (8)$$

$$\begin{aligned} C_A^{e} &= C_{A_1}^{e,s}(1 - \exp(-k_{A_1}^{e}t)) + C_{A_2}^{e,s}(1 - \exp(-k_{A_1}^{e}t)) \\ C_{A0}^{s} &= C_{A_1}^{e,s} + C_{A_2}^{e,s} \end{aligned} \quad (9)$$

The parameters of the *Potential* and *Exponential* models were calculated by fitting the experimental data of concentration in both phases as a function of time to the above expressions. In Appendix A.2 all the equations are described together with the definition of each term.

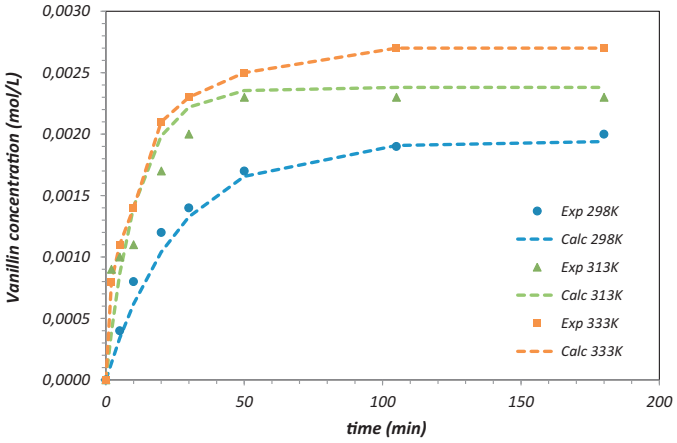

Fig. 2. Evolution of vanillin concentration on the organic phase along time. Influence of temperature. Rate of agitation: 300 rpm.

In the case of reaction in the presence of emulsion, the mass transport phenomena are coupled with the reactions. To derive the mass balances, in addition to the transport between the aqueous and organic phases, the reversible chemical transformation a reactant A (e.g. vanillin) into a product R (e.g. p-creosol) was taken into account. In these conditions, and considering first order reaction kinetics and a stable catalytic activity (i.e. no deactivation), the mass balances in the aqueous and organic phases are given respectively by:

$$\alpha^{w}\frac{dC_A^{w}}{dt} = -(k_1 + k_3)C_A^{w} + k_{-1}C_R^{w} - (K_A^{w}a)(C_A^{w} - C_A^{w,*}) \quad (10)$$

$$\alpha^{o}\frac{dC_A^{o}}{dt} = (K_A^{w}a)(C_A^{w} - C_A^{w,*}) = (K_A^{o}a)(C_A^{o,*} - C_A^{0}) \quad (11)$$

Similarly to the above cases, all the equations and the definition of each term that appears on these equations are described in Appendix A.3.

3. Results and discussion

3.1. Mass transport study for the single continuous interface case

Figs. 2–7 summarize the main results of the mass transport of vanillinrate for (VA) and p-creosol (MMF). Figs. 2–5 show, for both solutes, the influence of temperature and of stirring rate on the increase of the concentration in the oil phase with time. In the case

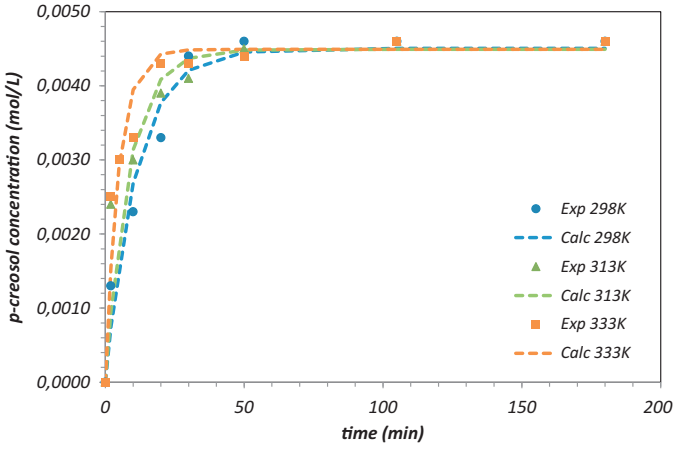

Fig. 3. Evolution of p-creosol concentration on the organic phasealong time. Influence of temperature. Rate of agitation: 300 rpm.

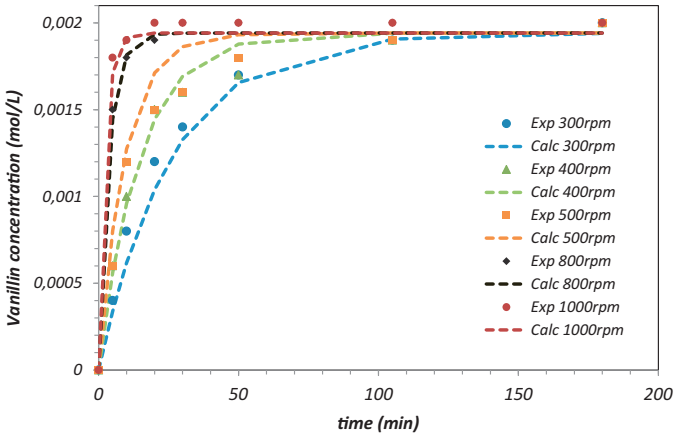

Fig. 4. Evolution of vanillin concentration on the organic phasealong time. Influence of stirring rate. Temperature: 298 K.

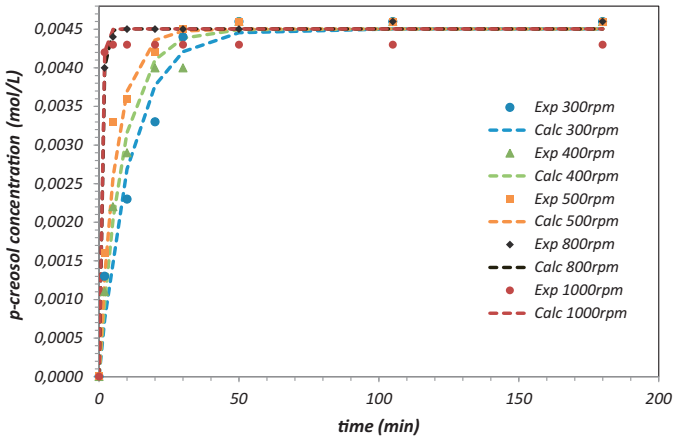

Fig. 5. Evolution of p-creosol concentration on the organic phasealong time. Influence of stirring rate. Temperature: 298 K.

of the study of the effect of the temperature, the stirring rate was maintained constant at 300 rpm, and in the case of the stirring rate effect, the temperature was 294 K. In all the cases, the initial concentration was zero and the concentration of the probe molecules increased, according to the model described by Eq. (3). In all the

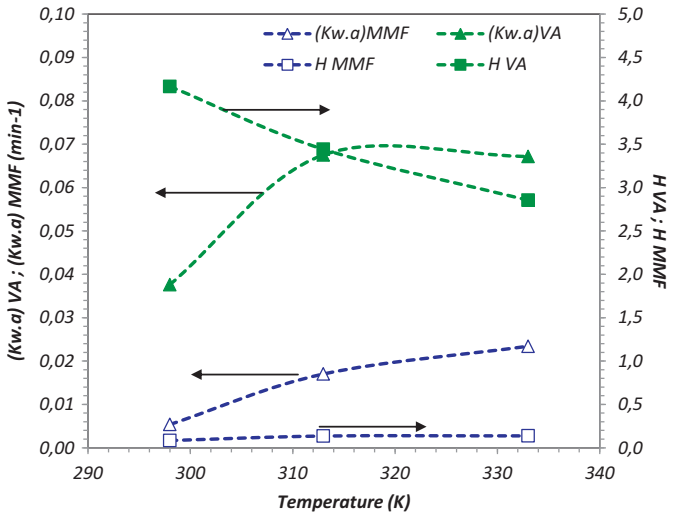

Fig. 6. Evolution of $(K_w a)$ and H with temperature for vanillin and p-creosol. Squared symbols: partition coefficients; triangles symbols: mass transport coefficients.

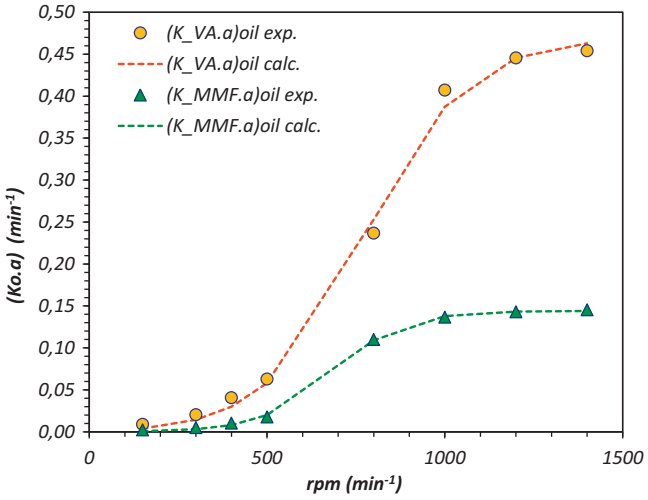

Fig. 7. Evolution of $(K_w a)$ with stirring rate for vanillin and p-creosol.

cases studied, the experimental data were very well fitted by this model.

The final concentration was determined by the combined effect of the solubility of the compound in the organic phase and by the mass transport coefficient, in which the rate of increase is given only by the value of the mass transport coefficient, (see Appendix A.1). As a general result, the operating temperature affects both, the partition coefficient, H_A, and the mass transport coefficient; however, the stirring rate only affects the mass transport coefficient. The effect of both operating variables on H_A and $(K_A^0 a)$ for both solutes, VA and MMF is shown in Figs. 6 and 7.

Regarding the effect of temperature (Table 1 and Fig. 6), an increase of the mass transport coefficient it is observed for both compounds when the kinetic energy of the molecules increased or the viscosity of the liquid mixture decreased. Both factors allow the mobility of the molecules, facilitating the transport across the interface. In average, the value of the mass transport coefficient of the VA is four times higher than the MMF. With respect to the partition coefficient, in the case of vanillin, H_{VA} diminishes with temperature because its solubility in the organic phase decreases. In the case of the p-creosol, the change in temperature does not seem to affect significantly the rate due to the low solubility of this molecule in decaline. In fact, the average ratio of H_{VA}/H_{MMF} is around 30, indicating that VA has a higher solubility in the aqueous phase. In fact, this enables the rapid transport of MMF, a product of the VA hydrogenation, from the aqueous phase to the oil phase, allowing simultaneous separation of the products after rapid formation.

The study of the effects of stirring rate (Fig. 7) in the range 150–1400 rpm covered conditions of transport by diffusion only (lowest stirring rates) to the case of transport by convection (high stirring rates). Above 500 rpm a clear increase in mass transport coefficients is observed for both compounds. Beyond 1000 rpm further increase is marginal and approaches an almost constant value. The mass transport coefficient for VA is three times higher than for MMF due to a higher diffusivity of vanillin in decalin.

Table 1
Influence of the temperature on mass transport coefficients for the single continuous interface case. Stirring rate = 300 rpm.

Temperature (K)	$(K_w a)_{MMF}$	H_{MMF}	$(K_w a)_{VA}$	H_{VA}
298	0.00538	0.084	0.03763	4.166
313	0.01701	0.135	0.06754	3.442
333	0.02342	0.137	0.06718	2.855

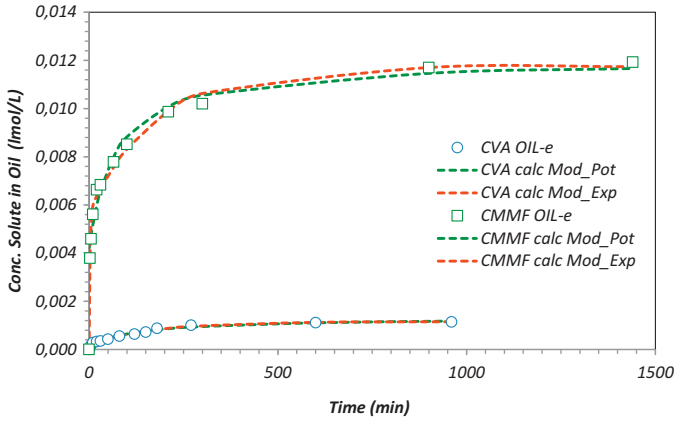

Fig. 8. Evolution of vanillin and p-creosol concentration with time. Oil phase of stable emulsion.

3.2. Mass transport study for stable emulsion

In this case, we have measured the evolution of vanillin and p-creosol concentrations with time for all phases involved in the stable emulsion composed of oil-in-water emulsion as well as excess free water. The aim of this experiment was to compare the results with those of the single continuous interface (i.e. no emulsion), in order to explore if the presence of a stable emulsion modifies significantly the values of the mass transport coefficients. The two empirical models described above, the *Potential* and *Exponential models* were used to obtain experimental mass transport coefficients between the free water and the two phases of the emulsion.

Figs. 8–10 show the evolution of vanillin and p-creosol concentrations with time for the oil phase in the table emulsion, water phase in stable emulsion (droplets) and for the excess free water out of the emulsion. The evolution of the concentrations indicates the transport from the free water phase to the oil phase and water droplets in the emulsion. Additionally, there is mass transport between the oil and the water droplets in the emulsion. In general, each compound migrates to the phase where it is more soluble. These phenomena take place until thermodynamic equilibrium is reached.

The fittings obtained with the *Potential Model* and the *Exponential Model* are included in the figures 8–10. Given that these models have a different number of parameters, the statistical discrimination has been carried out using the model selection criterion, MSC, defined as:

$$\mathrm{MSC} = \ln\left(\frac{\mathrm{SST}}{\mathrm{SSR}}\right) - \frac{2p}{n} \qquad (12)$$

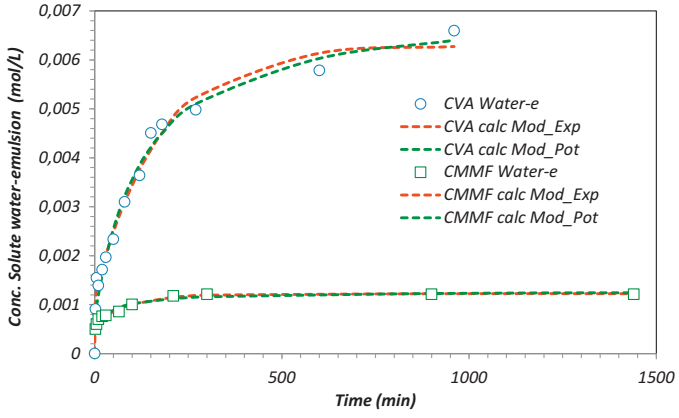

Fig. 9. Evolution of vanillin and p-creosol concentration with time. Water phase of stable emulsion.

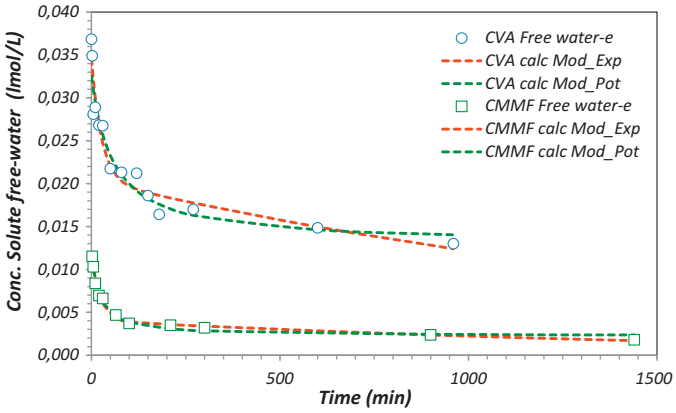

Fig. 10. Evolution of vanillin and p-creosol concentration with time. Water free phase of stable emulsion.

In the above equation, p represents the number of parameters of the model, and n the number of experimental points. The terms SSR and SST are respectively the sum of squared residuals and the sum of total squares defined by:

$$\mathrm{SSR} = \sum (C_{A,\mathrm{exp}} - C_{A,\mathrm{calc}})^2; \quad \mathrm{SST} = \sum (C_{A,\mathrm{exp}} - \overline{C_{A,\mathrm{exp}}})^2 \qquad (13)$$

This criterion indicates that the best model is one that gives the higher value of MSC. As can be seen in Figs. 8–10, both models fit very well the data, but in all the cases the MSC obtained with the *Exponential Model* is higher than with the *Potential model*. The parameter values obtained with the *Exponential Model* are presented in Table 2. The values of k_{VA1}, k_{VA2}, k_{MMF1} and k_{MMF2} correspond, in each transport phenomenon considered, to the two contributions assumed for the Exponential mode in the present study.

Overall, the resulting values for the mass transport coefficients of VA and MMF are in agreement with the highest solubility of VA in water and of MMF in decaline. These results showed that the first contribution (i.e. k_{VA1} and k_{MMF1}) is much more important than the second. For example, in the case of the transport of solute to the oil phase of the emulsion, the main contribution could be attributed to the direct transport from the free-water phase. The second contribution can be due to the transport of new droplets of water formed

Table 2
Mas transport parameters for the stable emulsion. *Exponential Model*. Stirring rate = 100 rpm.

To oil of the emulsion					
Vanillin (VA)			p-creosol (MMF)		
Parameter	Value	Stand. error	Parameter	Value	Stand. error
k_{VA1} (min^{-1})	0.2682	0.1145	k_{MMF1} (min^{-1})	0. 4165	0.0763
k_{VA2} (min^{-1})	0.0058	0.000530	k_{MMF2} (min^{-1})	0.0056	0.0009
To water of the emulsion					
Vanillin (VA)			p-creosol (MMF)		
Parameter	Value	Stand. error	Parameter	Value	Stand. error
k_{VA1} (min^{-1})	0.7282	0.4790	k_{MMF1} (min^{-1})	0.7395	0.1235
k_{VA2} (min^{-1})	0.0058	0.0006	k_{MMF2} (min^{-1})	0.0100	0.0013
From free water out of the emulsion					
Vanillin (VA)			p-creosol (MMF)		
Parameter	Value	Stand. error	Parameter	Value	Stand. error
k_{VA1} (min^{-1})	0.0375	0.0124	k_{MMF1} (min^{-1})	0.0450	0.0056
k_{VA2} (min^{-1})	0.0005	0.0002	k_{MMF2} (min^{-1})	0.0006	0.0002

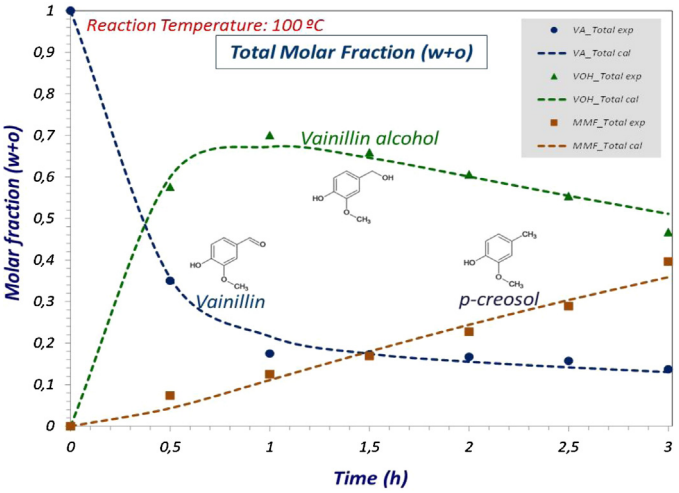

Fig. 11. Evolution of products and reactants with reaction time.

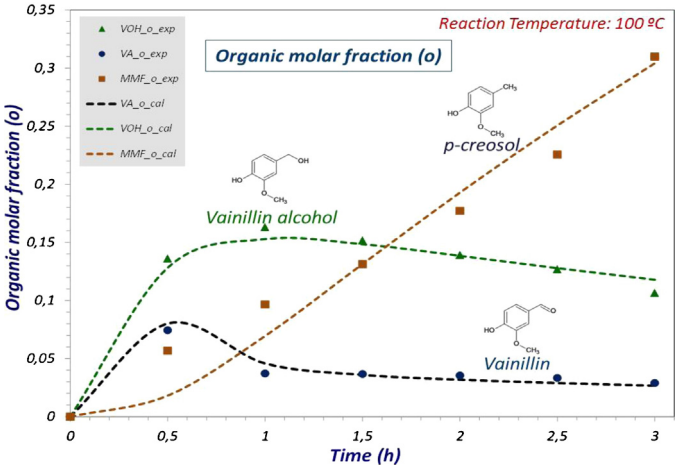

Fig. 13. Evolution of products and reactants with reaction time in oil phase.

during the process, having a high concentration of solute. In the case of the transport to the water droplets of the emulsion, the main contribution is ascribed to the transport from the oil. The second contribution can be caused by direct transport by local contact with the free-water phase. The global transport from the free-water phase is consequence of the above phenomena.

Finally, comparing these values with those obtained in the case of single continuous interface, it can be observed that, despite of the lower value of the stirring rate in the case of the experiment with the stable emulsions, the values of the coefficients (mainly k_{VA1} *and* k_{MMF1}) were higher than those of the single continuous interface. Therefore, the transport of the components is favoured in the case of a stable emulsion; attaining mass transport rates similar to the experiments carried out at 1000 rpm for single continuous interface. This can be explained by the very high interfacial area obtained when a stable emulsion is formed, and therefore the volumetric mass transport coefficient increases accordingly.

3.3. Catalytic reaction studies

Figs. 11–13 report the experimental results of vanillin conversion at 100 °C with Pd/CNT/SiO_2 catalytic nanohybrids obtained by Crossley et al. [8] in a batch reactor in an emulsion system. At this temperature, the only reaction that occurs at short times is the hydrogenation of the aldehyde (VA) to the vanillin alcohol (VOH). At longer times the alcohol is further converted to p-creosol (MMF) via hydrogenolysis [8]. Fig. 11 shows the total molar fraction of the three compounds measured in both phases, while Figs. 12 and 13 describe the evolution of the molar fractions in the aqueous and organic fractions, respectively. The evolution of the concentration is the result of a series of reactions. The ratio of concentrations observed in the aqueous and the organic fractions is determined from the partitioning coefficients. As it can be seen, the model described by Eq. (10) and (11) (see Appendix A.3) fits very well the experimental data. It is important to note that this model accurately captures the various phenomena involved in this complex process, i.e. several mass transport processes coupled with various consecutive reactions. Table 3 summarizes the kinetic constants, mass transport coefficients, and partitioning coefficients derived from the application of the model. The previous calculations of the mass transport coefficients and partitioning coefficients, allowed us to discriminate and calculate in a much more realistic form the intrinsic kinetic parameters (k_1, k_{-1} and k_2). Numerical simulations carried out with this model, (not shown here), indicate that an increase in conversion and selectivity is in fact produced as a consequence of the simultaneous mass transport limitations from the aqueous to the organic phase (Figs. 12 and 13).

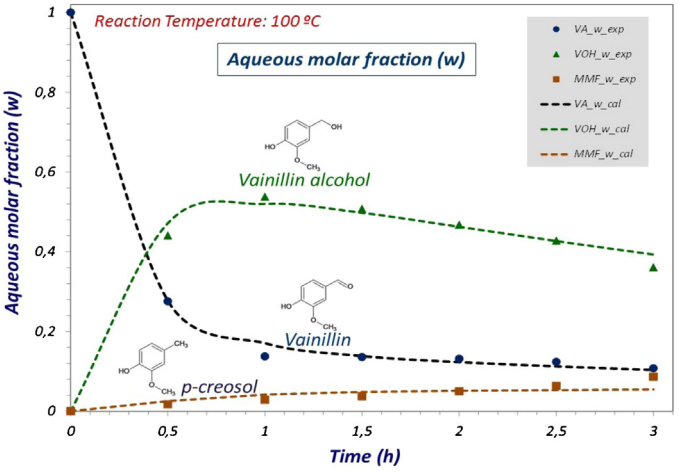

Fig. 12. Evolution of products and reactants with reaction time in water phase.

Table 3
Kinetic parameters of the vanillin conversion at 100 °C.

Parameter	Value	Standard error
k_1 (min^{-1})	3.229	0.647
k_{-1} (min^{-1})	0.797	0.092
k_2 (min^{-1})	0.272	0.095
$(K_{VA}{}^{w}a)$ (min^{-1})	9.455	0.908
$(K_{VOH}{}^{w}a)$ (min^{-1})	18.304	1.381
$(K_{MMF}{}^{w}a)$ (min^{-1})	3.078	0.611
$(K_{DMF}{}^{w}a)$ (min^{-1})	0.020	0.009
$(K_{VA}{}^{o}a)$ (min^{-1})	37.281	1.077
$(K_{VOH}{}^{o}a)$ (min^{-1})	62.001	6.070
$(K_{MMF}{}^{o}a)$ (min^{-1})	0.231	0.046
$(K_{DMF}{}^{o}a)$ (min^{-1})	0.003	0.001
H_{VA}	3.943	0.247
H_{VOH}	3.387	0.099
H_{MMF}	0.075	0.007
H_{DMF}	0.161	0.031

4. Conclusions

The mass transport phenomena are determinant factors in the global performance of reactions carried out in emulsions stabilized by solid nanohybrids of CNT/SiO_2 that can act as catalysts at the liquid–liquid interface.

We have measured the mass transport and partitioning coefficients of vanillin and its hydrogenolysis product, p-creosol, between aqueous and organic phases at different temperatures and stirring rates. The mathematical models developed in both cases studied, single continuous interface and stable w/o emulsions, enabled the calculation of the global mass transport and coefficients. In addition these models allowed us to quantify the effects of operating variables, such as temperature and stirring rate for the two cases considered in this study (i.e. single phase and emulsion). It was observed that the formation of stable emulsions markedly increases the value of the volumetric global mass transport coefficients due to the growth of the interfacial area. By increasing the mass transport coefficient with solid-particle stabilized emulsification the reaction rate can be greatly improved.

The mathematical model developed to quantify the conversion of vanillin in a stabilized emulsion successfully captures the main phenomena occurring in this system; (1) mass transport of the components between the phases of the emulsion, and (2) simultaneous reactions at the aqueous phase. This model fits accurately the evolution of the concentrations of all the components in both phases, and allows obtaining relevant kinetic data of the catalytic reactions in these unique operating conditions.

Acknowledgements

The authors acknowledge financial support from MINECO (Madrid, Spain)-FEDER, Project CTQ2010-16132, the Regional Government of Aragón(DGA-FSE) and the US Department of Energy (DOE/EPSCOR grant DESC-0004600)

Appendix A.

A.1. Modelling of mass transport in single continuous interface

The mass transport rate of the solute *A* between the both phases (water to oil) can be expressed in terms of overall mass transport coefficients as follows:

$$\frac{dC_A^{w}}{dt} = -(K_A^{w}a)(C_A^{w} - C_A^{w,*}) \tag{A.1-1}$$

$$\frac{dC_A^{o}}{dt} = -(K_A^{o}a)(C_A^{o,*} - C_A^{o}) \tag{A.1-2}$$

The term $(K_A^{w}a)$ is the overall volumetric mass transport coefficient referred to the water phase for the solute *A*, and $(K_A^{o}a)$ is the volumetric mass transport referred to oil phase. Denoting H_A as the partition coefficient of the solute *A* between the two phases at equilibrium, then the relationship between the equilibrium concentrations and mass transport coefficients are:

$$\begin{aligned} C_A^{w,*} &= H_A C_A^{o}; \quad C_A^{o,*} = \frac{C_A^{o}}{H_A} \\ (K_A^{o}a) &= H_A(K_A^{w}a) \end{aligned} \tag{A.1-3}$$

If the initial amount of moles added to the system (water + oil) in denoted as N_A^T, the distribution of moles in both phases can be calculated from the mass balance:

$$N_A^T = N_A^{o} + N_A^{w} = C_A^{o}V^{o} + C_A^{w}V^{w} \tag{A.1-4}$$

The above equation allows obtaining the relationship between the concentrations of A in both phases:

$$C_A^{o} = C_{A,T}^{o} - \alpha C_A^{w} \Leftrightarrow C_A^{w} = C_{A,T}^{w} - \beta C_A^{o} \tag{A.1-5}$$

In this equation the terms $C_{A,T}^{o}$, $C_{A,T}^{w}$, α and β are defined as:

$$C_{A,T}^{o} = \frac{N_A^T}{V^0}; \quad C_{A,T}^{w} = \frac{N_A^T}{V^w}; \quad \alpha = \frac{1}{\beta} = \frac{V^w}{V^0} \tag{A.1-6}$$

V^w and V^o are the volume of water phase and oil phase, respectively. $C_{A,T}^{w}$ and $C_{A,T}^{o}$ are the concentrations if all solute *A* would be dissolved in the water phase, or in the oil phase respectively. Substituting the above equations in the Eqs. (A.1-1) and (A.1-2), after integration is obtained the evolution of the concentration of *A* as function of time:

$$C_A^{o} = C_{A_\infty}^{o} - (C_{A_\infty}^{o} - C_{A_0}^{o})\exp(-(K_L a)_{A,\text{eff}}^{o} t) \tag{A.1-7}$$

In the above equation the terms $C_{A,\infty}^{o}$, $(K_A^{o}a)_{\text{eff}}$ are defined as:

$$C_{A\infty}^{o} = \left(\frac{C_{A,T}^{w}}{\beta + H_A}\right) \tag{A.1-8}$$

$$(K_A^{o}a)_{\text{eff}} = (K_A^{o}a)\left(\frac{\beta + H_A}{H_A}\right) \tag{A.1-9}$$

If the initial concentration in the oil phase is zero, i.e. $C_{A_0}^{o} = 0$, then, the Eq. (A.1-7) is simplified as:

$$C_A^{o} = C_{A\infty}^{o}(1 - \exp(-(K_A^{o}a)_{\text{eff}} t)) \tag{A.1-10}$$

By fitting the experimental data of concentration of *A* with time to the Eq. (A.1-10), the mass transport parameters, H_A and $(K_A^{o}.a)$, were calculated.

A.2. Modelling of mass transport in the particles-stabilized emulsion

In the case of formation of a stable emulsion three different phases were observed: (1) the "free-water" phase at the bottom of the vessel; (2) the "free-oil" phase at the upper part; and (3) the emulsion formed by water droplets dispersed in a continuous oil phase, at the middle of the vessel. In these conditions, the complete description of all the phenomena involved in mass transport in the presence of a stable emulsion is quite complex and therefore an empirical description of the phenomena has been assumed in this case. Two equations has been proposed; the *Potential* and the *Exponential* models.

The Potential model

The rates of mass transport equations proposed in this *Potential* model are:

$$\frac{dC_A^{f}}{dt} = -K_A^{f}(C_A^{f} - C_A^{f,s})^{n} \tag{A.2-1}$$

$$\frac{dC_A^{e}}{dt} = -K_A^{e}(C_A^{e,s} - C_A^{e})^{n} \tag{A.2-2}$$

The superscripts "f" and "e" refers to the free-water phase and to the emulsion respectively. It is assumed that the order of the *Potential Model*, *n*, is related to number of mass transport phenomena involved in the global process. Integrating the above equations for $n = 1$, the evolution with time of the concentrations on the "water-free" phase, and on the emulsion is given by:

$$C_A^{f} = C_A^{f,s} + (C_{A,0}^{f} - C_A^{f,s})\exp(-K_A^{f} t) \tag{A.2-3}$$

$$C_A^{e} = C_A^{e,s} - (C_A^{e,s} - C_{A,0}^{e})\exp(-K_A^{e} t) \tag{A.2-4}$$

For the case of $n > 1$, the corresponding integrated equations for both phases are:

$$C_A^{\mathrm{f}} = C_A^{\mathrm{f,s}} + \frac{(C_{A,0}^{\mathrm{f}} - C_A^{\mathrm{f,s}})}{(1 + k_{A,\mathrm{eff}}^{\mathrm{f}} t)^d} \quad \text{(A.2-5)}$$

$$C_A^{\mathrm{e}} = C_A^{\mathrm{e,s}} + \frac{(C_A^{\mathrm{e,s}} - C_{A,0}^{\mathrm{e}})}{(1 + k_{A,\mathrm{eff}}^{\mathrm{e}} t)^d} \quad \text{(A.2-6)}$$

In the above equations, the terms d, $k_{A,\mathrm{eff}}^{\mathrm{f}}$ and $k_{A,\mathrm{eff}}^{\mathrm{f}}$ are given by:

$$d = \frac{1}{(n-1)} \quad \text{(A.2-7)}$$

$$k_{A,\mathrm{eff}}^{\mathrm{f}} = \frac{(n-1)K_A^{\mathrm{f}}}{(C_{A,0}^{\mathrm{f}} - C_A^{\mathrm{f,s}})^{(1-n)}} \quad \text{(A.2-8)}$$

$$k_{A,\mathrm{eff}}^{\mathrm{e}} = \frac{(n-1)K_A^{\mathrm{f}}}{(C_A^{\mathrm{e,s}} - C_{A,0}^{\mathrm{e}})^{(1-n)}} \quad \text{(A.2-9)}$$

Similarly, by fitting the experimental data of the concentration of A as a function of time to the Eqs. (A.2-3)–(A.2-6), the mass transport parameters of the *Potential model* (K_A^{f}, K_A^{s}, $C_A^{\mathrm{f,s}}$, $C_A^{\mathrm{e,s}}$ and n) were calculated.Exponential model

In this model the mass transport is described as a sum of exponential functions. Similarly to the *Potential model*, the number of the exponentials, n, is related to the number mass transport phenomena involved in the global process. According to this model the evolution of the concentration in both phases can be described as follows:

$$C_A^{\mathrm{f}} = \sum_{i=1}^{n} C_{i,0}^{\mathrm{f}} \exp(-k_i^{\mathrm{f}} t); \quad C_{A,0}^{\mathrm{f}} = \sum_{i=1}^{n} C_{i,0}^{\mathrm{f}} \quad \text{(A.2-10)}$$

$$C_A^{\mathrm{e}} = \sum_{i=1}^{n} C_i^{\mathrm{e,s}} (1 - \exp(-k_i^{\mathrm{e}} t)); \quad C_A^{\mathrm{s}} = \sum_{i=1}^{n} C_{i,0}^{\mathrm{e,s}} \quad \text{(A.2-11)}$$

Again, by fitting the experimental data of concentration of A with time to the Eqs. (A.2-3)–(A.2-6), the mass transport parameters of the *Exponential model* ($C_{i,0}^{\mathrm{f}}$, k_i^{f}, $C_i^{\mathrm{e,s}}$ and k_i^{e}) were calculated.

A.3. Kinetic modelling of vanillin conversion in particles-stabilized emulsions

The following is the simplified reaction scheme for the conversion of vanillin that has been assumed:

$$\mathrm{VA} \overset{k_1, k_{1-}}{\longleftrightarrow} \mathrm{VOH} \xrightarrow{k_2} \mathrm{MMF}$$
$$\mathrm{VA} \overset{k_3}{\longleftrightarrow} \mathrm{DMH}$$

The acronyms used are: VA: vanillin (3-methoxy-4-hydroxybenzaldehyde); VOH: vanillin alcohol (3-methoxy-4-hydroxybenzyl alcohol); MMF: p-creosol (2-methoxy-4-methyl phenol); DMF: guaiacol (2-methoxy phenol). The following assumptions have been made (i) the reactions occur only in the water side of the liquid–liquid interface inside the emulsion, (ii) all the reactions are considered of 1st order, (iii) the concentration in all the water droplets is the same, (iv) the concentration of the reacting species in the oil phase is homogeneous, i.e. the concentrations in the oil continuous phase and in the oil inside the emulsion are equal, (v) simultaneous mass transport (water to oil) of the components as they react, (vi) the catalyst does not suffer deactivation, and (vii) the internal mass transport limitations are negligible. In order to avoid an strong increase of the number of parameters during the simulation of the mass transfer-reaction studies, we have assumed, as a first approach, that the reaction is of first order and that the catalyst is stable and do not suffers any phenomenon of deactivation. More detailed studies of the reaction mechanisms (including all the phases present in this complex system) should conduce to the development of more realistic kinetic expressions. Nevertheless, the approach followed is valid to compare the relative importance of the mass transfer rate with respect to the intrinsic kinetic rate, and also to compare the performance of several nanohybrids.

In these conditions the mass balances for each compound are:

(1) Mass balance for the vanillin in aqueous and organic phases:

$$\alpha^{\mathrm{w}} \frac{dC_{\mathrm{VA}}^{\mathrm{w}}}{dt} = -(k_1 + k_3) C_{\mathrm{VA}}^{\mathrm{w}} + k_{-1} C_{\mathrm{VOH}}^{\mathrm{w}} - (K_{\mathrm{VA}}^{\mathrm{w}} a)(C_{\mathrm{VA}}^{\mathrm{w}} - C_{\mathrm{VA}}^{\mathrm{w1*}}) \quad \text{(A.3-1)}$$

$$\alpha^{\mathrm{o}} \frac{dC_{\mathrm{VA}}^{\mathrm{o}}}{dt} = (K_{\mathrm{VA}}^{\mathrm{w}} a)(C_{\mathrm{VA}}^{\mathrm{w}} - C_{\mathrm{VA}}^{\mathrm{w,*}}) = (K_{\mathrm{VA}}^{\mathrm{o}} a)(C_{\mathrm{VA}}^{\mathrm{o,*}} - C_{\mathrm{VA}}^{\mathrm{0}}) \quad \text{(A.3-2)}$$

$$C_{\mathrm{VA}}^{\mathrm{w}} = H_{\mathrm{VA}} C_{\mathrm{VA}}^{\mathrm{o,*}}; \quad C_{\mathrm{VA}}^{\mathrm{w,*}} = H_{\mathrm{VA}} C_{\mathrm{VA}}^{\mathrm{o}} \quad \text{(A.3-3)}$$

(2) Mass balance for the vanillin alcohol in aqueous and organic phases:

$$\alpha^{\mathrm{w}} \frac{dC_{\mathrm{VOH}}^{\mathrm{w}}}{dt} = k_1 C_{\mathrm{VA}}^{\mathrm{w}} - (k_2 + k_{-1}) C_{\mathrm{VOH}}^{\mathrm{w}} - (k_{\mathrm{VOH}}^{\mathrm{w}} a)(C_{\mathrm{VOH}}^{\mathrm{w}} - C_{\mathrm{VOH}}^{\mathrm{w,*}}) \quad \text{(A.3-4)}$$

$$\alpha^{\mathrm{o}} \frac{dC_{\mathrm{VOH}}^{\mathrm{o}}}{dt} = (K_{\mathrm{VOH}}^{\mathrm{w}} a)(C_{\mathrm{VOH}}^{\mathrm{w}} - C_{\mathrm{VOH}}^{\mathrm{w,o}}) = (K_{\mathrm{VOH}}^{\mathrm{o}} a)(C_{\mathrm{VOH}}^{\mathrm{o,*}} - C_{\mathrm{VOH}}^{\mathrm{o}}) \quad \text{(A.3-5)}$$

$$C_{\mathrm{VOH}}^{\mathrm{w,*}} = H_{\mathrm{VOH}} C_{\mathrm{VOH}}^{\mathrm{o}}; \quad C_{\mathrm{VOH}}^{\mathrm{w}} = H_{\mathrm{VOH}} C_{\mathrm{VOH}}^{\mathrm{o,*}} \quad \text{(A.3-6)}$$

(3) Mass balance for the 2-methoxy-4-methyl phenol in aqueous and organic phases:

$$\alpha^{\mathrm{w}} \frac{dC_{\mathrm{MMF}}^{\mathrm{w}}}{dt} = k_2 C_{\mathrm{VOH}}^{\mathrm{w}} - (K_{\mathrm{MMF}}^{\mathrm{w}} a)(C_{\mathrm{MMF}}^{\mathrm{w}} - C_{\mathrm{MMF}}^{\mathrm{w,*}}) \quad \text{(A.3-7)}$$

$$\alpha^{\mathrm{o}} \frac{dC_{\mathrm{MMF}}^{\mathrm{o}}}{dt} = (K_{\mathrm{MMF}}^{\mathrm{w}} a)(C_{\mathrm{MMF}}^{\mathrm{w}} - C_{\mathrm{MMF}}^{\mathrm{w,*}}) = (k_{\mathrm{MMF}}^{\mathrm{o}} a)(C_{\mathrm{MMF}}^{\mathrm{o,*}} - C_{\mathrm{MMF}}^{\mathrm{o}}) \quad \text{(A.3-8)}$$

$$C_{\mathrm{MF}}^{\mathrm{w,*}} = H_{\mathrm{MMF}} C_{\mathrm{MMF}}^{\mathrm{o}}; \quad C_{\mathrm{MMF}}^{\mathrm{w}} = H_{\mathrm{MMF}} C_{\mathrm{MMF}}^{\mathrm{o,*}} \quad \text{(A.3-9)}$$

(4) Mass balance for the 2-methoxy-phenol in aqueous and organic phases:

$$\alpha^{\mathrm{w}} \frac{dC_{\mathrm{DMF}}^{\mathrm{w}}}{dt} = k_3 C_{\mathrm{VA}}^{\mathrm{w}} - (K_{\mathrm{DMF}}^{\mathrm{w}} a)(C_{\mathrm{DMF}}^{\mathrm{w}} - C_{\mathrm{DMF}}^{\mathrm{w,*}}) \quad \text{(A.3-10)}$$

$$\alpha^{\mathrm{o}} \frac{dC_{\mathrm{DMF}}^{\mathrm{o}}}{dt} = (K_{\mathrm{DMF}}^{\mathrm{w}} a)(C_{\mathrm{DMF}}^{\mathrm{w}} - C_{\mathrm{DMF}}^{\mathrm{w,*}}) = (K_{\mathrm{DMF}}^{\mathrm{o}} a)(C_{\mathrm{DMF}}^{\mathrm{o,*}} - C_{\mathrm{DMF}}^{\mathrm{o}}) \quad \text{(A.3-11)}$$

$$C_{\mathrm{DMF}}^{\mathrm{w,*}} = H_{\mathrm{DMF}} C_{\mathrm{DMF}}^{\mathrm{o}}; \quad C_{\mathrm{DMF}}^{\mathrm{w}} = H_{\mathrm{DMF}} C_{\mathrm{DMF}}^{\mathrm{o,*}} \quad \text{(A.3-12)}$$

(5) Global mass balance:

$$(N_{\mathrm{VA}})_0 = \sum_i (N_i)_t = (N_{\mathrm{VA}})_t + (N_{\mathrm{VOH}})_t + (N_{\mathrm{MMF}})_t + (N_{\mathrm{DMF}})_t \quad \text{(A.3-13)}$$

$$(N_i)_t = N_i^{\mathrm{w}} + N_i^{\mathrm{o}} = V^{\mathrm{w}} C_i^{\mathrm{w}} + V^{\mathrm{o}} C_i^{\mathrm{o}} \quad \text{(A.3-14)}$$

$$\alpha^{\mathrm{w}} = \frac{V^{\mathrm{w}}}{V^{\mathrm{o}} + V^{\mathrm{w}}}; \quad \alpha^{\mathrm{o}} = \frac{V^{\mathrm{o}}}{V^{\mathrm{o}} + V^{\mathrm{w}}} \quad \text{(A.3-15)}$$

All the concentrations are expressed in molar fractions. The terms ($K_i^w a$) and ($K_i^o a$) are the volumetric global mass transport coefficients in the aqueous and organic phases, respectively. Units: time^{-1}. H_{VA}, H_{VOH}, H_{DMF} and H_{MMF} are the partition coefficients of the reacting molecules between the aqueous and organic phases.

The above set of differential and algebraic equations has been solved numerically using the fourth-order Runge–Kutta method, coupled with a Levenberg–Marquardt routine for the minimization of the objective function by non-linear regression.

References

[1] G.W. Huber, J.A. Dumesic, Catalysis Today 111 (2006) 119–132.
[2] A. Demirbas, Biorefineries: For Biomass Upgrading Facilities, vol. 49, Springer, London, 2010, pp. 75–91.
[3] J. Kawahara, T. Ohmori, T. Ohkubo, S. Hattori, M. Kawamura, Anal. Biochem. 201 (1992) 94–98.
[4] M. Makosza, Pure Appl. Chem. 72 (2000) 5.
[5] S.D. Naik, L.K. Doraiswamv, AIChE J. 44 (1998) 35.
[6] C.M. Starks, J. Am. Chem. Soc. C 93 (1971) 5.
[7] P. Finkle, H.D. Draper, J.H. Hildebrand, J. Am. Chem. Soc. 45 (1923) 2780–2788.
[8] S. Crossley, J. Faria, M. Shen, D.E. Resasco, Science 327 (2010) 68–72.
[9] B.P. Binks, S.O. Lumsdon, Langmuir 16 (2000) 8622–8631.
[10] M. Shen, D.E. Resasco, Langmuir 25 (2009) 10843–10851.
[11] M.P. Ruiz, J. Faria, M. Shen, S. Drexler, T. Prasomsri, D.E. Resasco, ChemSusChem 4 (2011) 964–974.
[12] A. Bachinger, G. Kickelbick, Monatsh. Chem. 141 (2010) 685–690.
[13] B.P. Binks, Curr. Opin. Colloid Interface Sci. 7 (2002) 21.
[14] B.P. Binks, J.H. Clint, Langmuir 18 (2002) 1270–1273.
[15] B.P. Binks, P.D.I. Fletcher, B.L. Holt, J. Parker, P. Beaussoubre, K. Wong, Phys. Chem. Chem. Phys. 12 (2010) 11967–11974.
[16] J. Frelichowska, M.A. Bolzinger, Y. Chevalier, Colloids Surf. A 343 (2009) 70–74.
[17] S.U. Pickering, J. Chem. Soc. 91 (1907) 2001–2021.
[18] R.J. Madon, E. Iglesia, J. Mol. Catal. A Chem. 163 (2000) 189–204.
[19] R.J. Madon, J.P. O'Connell, M. Boudart, AIChE J. 24 (1978) 904–911.
[20] S. Mukherjee, M.A. Vannice, J. Catal. 243 (2006) 108–130.
[21] S. Mukherjee, M.A. Vannice, J. Catal. 243 (2006) 131–148.
[22] J. Struijk, M. d'Angremond, W.J.M. Lucas-de Regt, J.J.F. Scholten, Appl. Catal. A 83 (1992) 263–295.
[23] B.P. Binks, J.H. Clint, P.D.I. Fletcher, S. Rippon, S.D. Lubetkin, P.J. Mulqueen, Langmuir 14 (1998) 5402–5411.
[24] B.P. Binks, P.D.I. Fletcher, B.L. Holt, O. Kuc, P. Beaussoubre, K. Wong, Phys. Chem. Chem. Phys. 12 (2010) 2219–2226.
[25] B.P. Binks, J.H. Clint, P.D.I. Fletcher, S. Rippon, S.D. Lubetkin, P.J. Mulqueen, Langmuir 15 (1999) 4495–4501.
[26] J. Frelichowska, M.A. Bolzinger, Y. Chevalier, J. Colloid Interface Sci. 351 (2010) 348–356.
[27] B.R. Midmore, J. Colloid Interface Sci. 213 (1999) 352–359.
[28] T. Ohtake, T. Hano, K. Takagi, F. Nakashio, J. Chem. Eng. Jpn. 20 (1987) 443–447.
[29] D.J. Kraft, B. Luigjes, J.W.J. de Folter, A.P. Philipse, W.K. Kegel, J. Physical Chemistry B 114 (2010) 12257–12263.
[30] C.Y. Wang, R. Yang, Y.H. Chen, Z. Tong, CJCU 31 (2010) 864–866.
[31] S. Wang, Y.J. He, Y. Zou, Particuology 8 (2010) 390–393.
[32] F. Yang, J. Wang, Q. Lan, D.J. Sun, C.X. Li, Prog. Chem 21 (2009) 1418–1426.
[33] J. Faria, M.P. Ruiz, D.E. Resasco, Adv. Synth. Catal 352 (2010) 2359–2364.
[34] A. Kollmer, A. Schmid, P.R. von Rohr, B. Sonnleitner, Bioprocess Engineering 20 (1999) 441–448.
[35] C.L.M. Marcelis, M. van Leeuwen, H.G. Polderman, A.J.H. Janssen, G. Lettinga, Biochem. Eng. J 16 (2003) 253–264.
[36] T. Prasomsri, D. Shi, D.E. Resasco, Chem. Phys. Lett 497 (2010) 103–107.